Flow of a Falling Film into a Pool

Complete interfacial profiles are generated for the gravity flow of a thin film into a stagnant pool. The profiles show standing waves and a rapid thinning of the film just above the static meniscus over the pool. Such effects are encountered, for example, at the bottom of wetted wall columns.

KENNETH J. RUSCHAK

Research Laboratories
Eastman Kodak Company
Rochester, New York 14650

SCOPE

Standing waves are observed where a liquid film or jet enters a relatively large pool. Examples include flow at the bottom of a wetted wall column and flow at the rear of long bubbles in tubes. These exit effects must sometimes be considered in equipment design. Although several analyses of exiting flows have been reported, predictions of complete interfacial profiles have yet to be made.

The purpose of this study is to elucidate the mechanism of film flow down a vertical wall into a relatively large pool of arbitrary geometry and to make predictions of the flow field and interfacial shape. Another aim is to illustrate a straightforward method for simplifying and solving the governing equations which can readily be generalized to situations where the wall is not vertical, for example, or where the interface is stagnant.

CONCLUSIONS AND SIGNIFICANCE

The film thins in a transition zone between the fully developed flow upstream and the reservoir by the following mechanism. Far upstream the film thickness is uniform, and the pressure in the liquid is atmospheric; however, the pressure beneath the curved and essentially static meniscus over the pool is subatmospheric because of the capillary pressure drop across the interface. Consequently, there is a pressure gradient in the transition zone. The film thins to develop a horizontal shear stress gradient to balance this capillary pressure gradient, which is generally larger than a hydrostatic pressure gradient. At low flow rates, the film thickness in the transition zone is much smaller than the film thickness far upstream. For a given upstream film thickness, increasing Reynolds number tends initially to decrease the minimum film thickness. A series of standing waves, whose amplitude rapidly decreases in the upstream direction, forms above the transition zone.

Although there are three distinct regions, one set of simplified equations can predict the features and extent of exiting flow. This set of simplified equations is arrived at by discarding only those terms in the complete set of governing equations which are unimportant over the entire flow domain. Patching schemes or singular perturbation methods are much more difficult to use when characteristic length scales are disparate in three zones.

Hydrodynamic end effects for flow into a stagnant pool have been reported by several investigators. Cook and Clark (1973) described the standing waves which form at the bottom of wetted wall columns whether or not surface active agents are present. Merson and Quinn (1964, 1965) established that surfactants collect at the interface, forming a stationary film which can be centimeters in length. When such a film forms, small ripples of the interface just upstream mark its extent (Lynn et al., 1955*b*; Mockros and Krone, 1968). Lynn et al. (1955*a*), Nysing et al. (1958), and Nijsing et al. (1959), who employed surfactants to control surface waves, made corrections for hydrodynamic end effects in their mass transfer studies. Cullen and Davidson (1957) described analogous end effects for liquid jets, and Bretherton (1961) found standing waves at the rear of long bubbles rising in capillary tubes.

Here, the hydrodynamics of the gravity driven flow of a film down a vertical wall into an essentially stagnant pool is studied. The upstream thickness of the film is presumed small in comparison to the characteristic dimension of the pool. In this situation, dynamic forces are important only in the descending thin film, and the pool is capped by a static meniscus. Estimates show that at the lowest flow rates there must be three disparate horizontal (cross film) length scales. The smallest length scale occurs in the transition zone between the pool and the developed flow upstream. Here, the film thins, and its average velocity increases as the pressure in the film drops from atmospheric pressure to that found beneath the curved static meniscus.

The governing equations of capillary hydrodynamics are simplified by casting off terms which are not important in any of the three zones. The numerical solution generated for the simplified equations is exact when the Reynolds number is zero and approximate when the Reynolds number is nonzero. In this way, complete interfacial profiles are generated for this flow which exhibit standing waves, and the expected thinning of the film just above the pool is confirmed. The flow in the transition zone is influenced by any changes in pool geometry which affect the static meniscus. The analyses closest to that which follows are by Bretherton (1961) and by Wilkes and Nedderman (1962).

0001-1541-78-9636-0705-$00.75.

GOVERNING EQUATIONS

A Newtonian liquid flows down a vertical wall at the volumetric flow rate per unit width Q into a pool or reservoir. Far upstream the flow is fully developed, and the film thickness D equals $(3\mu Q/\rho G)^{1/3}$. The flow is steady and two dimensional.

An X-Y Cartesian coordinate system has its X axis on the wall, with X increasing in the downstream direction. Dimensionless coordinates x and y are in units of the capillary length C, where $C = (\sigma/\rho G)^{1/2}$ is the characteristic dimension of static menisci whose shape is influenced by gravity. The components of the velocity vector are made dimensionless with $\rho GD^2/\mu$, the characteristic speed far upstream, and the pressure over atmospheric pressure is made dimensionless with ρGC, a measure of hydrostatic pressure. The dimensionless x and y components of velocity are u and v, respectively, and the dimensionless pressure is p. The film profile is given by $y = h(x)$.

The Navier-Stokes equation and boundary conditions then take the form

$$Rd^{-1}[uu_x + vu_y] = -d^{-2}p_x + u_{yy} + u_{xx} + d^{-2} \quad (1)$$
$$Rd^{-1}[uv_x + vv_y] = -d^{-2}p_y + v_{yy} + v_{xx}$$

$$u_x + v_y = 0$$

$$\left.\begin{aligned} &p + 2d^2\, u_x(1 + h_x^2)/(1 - h_x^2) + \kappa = 0 \\ &(u_y + v_x)(1 - h_x^2) - 4h_x u_x = 0 \\ &v = h_x u \end{aligned}\right\} y = h(x)$$

$$u \to d^{-2}\left(dy - \frac{1}{2}y^2\right), \quad v \to 0, \quad h \to d \quad (x \to -\infty)$$

$$u = 0, \quad v = 0 \quad (y = 0)$$

$R = \rho^2 GD^3/\mu^2 = 3\rho Q/\mu$ is the Reynolds number, and $d = D/C$ is the ratio of the film thickness far upstream to the capillary length. The curvature of the film profile is $\kappa = h_{xx}(1 + h_x^2)^{-3/2}$. In the special case considered below, the downstream boundary condition comes from specification of the static meniscus which caps the pool.

MECHANISM FOR FILM THINNING IN THE EXIT REGION

The thickness of the film upstream D is considered to be small in comparison with the characteristic dimension of the pool. Consequently, dynamic effects are negligible in the reservoir, and the pool of liquid is well described by a hydrostatic pressure field beneath a static meniscus. Although the pressure in the film is atmospheric far upstream it is below atmospheric by the amount σ/E at the top of the nearly hydrostatic region, where E is the radius of curvature of the static meniscus close to the wall. A pressure gradient therefore exists in the transition zone between the region of fully developed flow upstream and the hydrostatic pool. In the case of nearly rectilinear, low Reynolds number flow, a viscous stress gradient across the film will balance this pressure gradient. The following estimates predict that the film thins in the transition zone to produce a viscous stress gradient large enough to balance the capillary pressure gradient.

In the transition zone, let the characteristic vertical dimension be $\hat{X}$ and the characteristic film thickness be $\hat{Y}$. The capillary pressure gradient in the film $\sigma/E\hat{X}$ is dictated by the rate of change of profile curvature $\hat{Y}/\hat{X}^3$:

$$E\hat{Y} \sim \hat{X}^2 \quad (2)$$

This pressure gradient is balanced by the cross film gradient of the shear stress, which is estimated for nearly rectilinear flow:

$$\sigma/E\hat{X} \sim \mu Q/\hat{Y}^3 \quad (3)$$

Together, these two results imply that

$$\hat{Y}/D \sim E^{3/5}D^{1/5}/C^{4/5} \quad (4)$$

$$\hat{X}/D \sim E^{4/5}/D^{2/5}C^{2/5} \quad (5)$$

When the flow rate is sufficiently small, therefore, the film is estimated to be much thinner in the transition zone than it is far upstream. Additionally, it is anticipated that the film thickness in the transition zone is less, for identical flow rates, the more highly curved is the static meniscus over the pool. Finally, comparison of the estimate obtained above for the capillary pressure gradient in the transition zone with a hydrostatic pressure gradient suggests that gravity is of secondary importance where the film is thinnest.

SIMPLIFICATION OF THE GOVERNING EQUATIONS

When the flow rate is so low that the characteristic dimension of the pool into which the film flows is much larger than D, the film thickness far upstream, dynamic forces are of secondary importance in the pool, and the liquid/air interface is a static meniscus. The equations of capillary hydrostatics follow from Equations (1) when all dynamic terms are omitted:

$$0 = -p_x + 1; \quad 0 = -p_y \quad (6a, b)$$

$$p + \kappa = 0 \quad (y = h) \quad (6c)$$

The integration of Equations (6) gives rise to a hydrostatic pressure field and a one-parameter family of static menisci. A convenient identifying parameter is given by

$$\alpha = \kappa^2 + 2h_x(1 + h_x^2)^{-1/2} \quad (7)$$

That α is a constant when Equations (6) hold is easily verified upon differentiation.

Because the absolute value of the final term in Equation (7) is no greater than 2, α is essentially the square of the curvature of highly curved menisci. For the special case of an unbounded reservoir, $\kappa \to 0$ as $h_x \to \infty$, and $\alpha = 2$. For $\alpha < 2$, the meniscus has an inflection point, and α then relates to the slope at this point. When $\alpha = 0$, the slope of the meniscus is zero at the inflection point. Those static menisci for which α is negative are not encountered in what follows.

Dynamic forces are important in the thin film above the pool. If the slope there is everywhere small, then $u \sim d/h$, $v \sim h_x u$, and the flow is nearly rectilinear. On the assumption that each y differentiation of an independent variable is of order unity, while each x differentiation is of order $||h_x|| << 1$, it follows that the dominant terms of Equation (1) are

$$Rd^{-1}(uu_x + vu_y) = -d^{-2}p_x + u_{yy} + d^{-2} \quad (8a)$$

$$0 = d^{-2}p_y; \quad u_x + v_y = 0 \quad (8b, c)$$

$$p + \kappa = 0, \quad u_y = 0, \quad v = h_x u \quad (y = h) \quad (8d, e, f)$$

$$u \to d^{-2}\left[dy - \frac{1}{2}y^2\right], \quad v \to 0, \quad h \to d \quad (x \to \infty) \quad (8g, h, i)$$

$$u = 0, \quad v = 0 \quad (y = 0) \quad (8j, k)$$

In Equation (8d) κ, the profile curvature, should be approximated by h_{xx}.

To obtain a set of governing equations which can describe both the dynamic flow in the film and the hydrostatic pool, the above two sets of simplified equations are combined. This requires only that in Equation (8*d*) κ not be replaced by h_{xx}. The expectation is that the resulting equations, which contain all the terms estimated to be important in one region or another, can generate an approximate solution over the entire domain.

SOLUTION PROCEDURES

An approximate solution of Equations (8) is sought using the technique of weighted residuals, method of moments (Finlayson, 1972). The lowest-order polynomial representation of the x component of velocity is

$$u = (d/h^3)\left(hy - \frac{1}{2}y^2\right) \tag{9}$$

It satisfies boundary conditions (8*e*), (8*g*), and (8*j*). This form for u is exact when the Reynolds number is zero. The concomitant representation of the y component of velocity is

$$v = (y/h)h_x u \tag{10}$$

which obeys boundary conditions (8*h*) and (8*k*). Together, these expressions for u and v satisfy the continuity Equation (8*c*) and the kinematic boundary condition (8*f*). According to Equation (8*b*), the pressure is uniform across the film, and consequently Equation (8*d*) gives the pressure in the film. Substitution for p, u, and v in Equation (8*a*) yields a residual which depends upon y only if the Reynolds number is nonzero. When the weighted integral of this residual across the film, with unity as the weighting function, is set to zero, the following ordinary differential equation results for the film profile:

$$0 = h_{xxx}(1 + h_x^2)^{-3/2} - 3h_x h_{xx}^2(1 + h_x^2)^{-5/2} + 1 - (d/h)^3 \cdot (1 - 2Rh_x/15) \tag{11}$$

Two boundary conditions determine the solution of Equation (11) to within a vertical translation. First, $h \to d$ as $x \to -\infty$. The profile is then fixed by specifying α; that is, the static meniscus which describes the surface of the pool is specified. For instance, $\alpha = 2$ for a pool of unbounded extent.

RESULTS

Numerical integrations of Equation (11) confirm expectations. The transition region for one profile is plotted in Figure 1. Here, $d = 10^{-4}$, $R = 0$, and $\alpha = 2$. The three horizontal length scales of the flow are evident. Above the transition region is a series of standing waves whose amplitude diminishes rapidly in the upstream direction.

These gross features of the flow can be explained as follows. Static menisci with small slope and curvature near the wall (α near zero) curve in toward the wall as x increases, while static menisci with small slope and large curvature near the wall (α of magnitude unity or greater) curve away from the wall as x increases. Therefore, far upstream, where the slope and curvature of the film profile are small, the meniscus turns back to the wall once the film thickens and dynamic forces diminish in importance. The average velocity of the thinning film increases, as does the shear stress gradient across the film. As a result, the pressure in the film falls, and the meniscus eventually curves away from the wall. This process recurs with increasing amplitude until the curvature of the film profile at a trough becomes so large that the dynamic meniscus blends with a static meniscus which curves away from the wall. The film then ends in a hydrostatic pool.

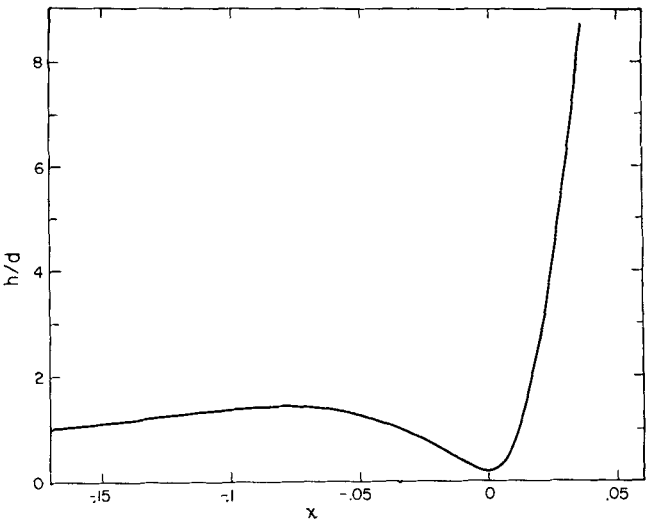

Fig. 1. Film profile for $d = 10^{-4}$, $\alpha = 2$, $R = 0$.

In Figure 2 are plots for several values of d of the minimum thickness of the film, computed as a fraction of the upstream film thickness, as a function of α, which identifies the static meniscus over the reservoir. The Reynolds number is zero, and so the numerical solution of the simplified equations is exact. Also shown are plots of the maximum thickness of the ripple immediately upstream from the transition zone. As α becomes larger, the curvature of the static meniscus increases, and the minimum film thickness decreases. This is expected [see Equation (4)] because a larger pressure drop occurs across the transition zone as the curvature of the static meniscus increases. Moreover, the plots confirm that the minimum fractional film thickness is $0(d^{1/5})$ as $d \to 0$. There are indeed three horizontal length scales in the limit $d \to 0$.

In Figure 3, the initial effects of increasing Reynolds number are shown for the case $d = 0.01$. When the Reynolds number is nonzero, the simplified equations are solved only approximately. Nevertheless, the calculations should establish the Reynolds number at which inertia

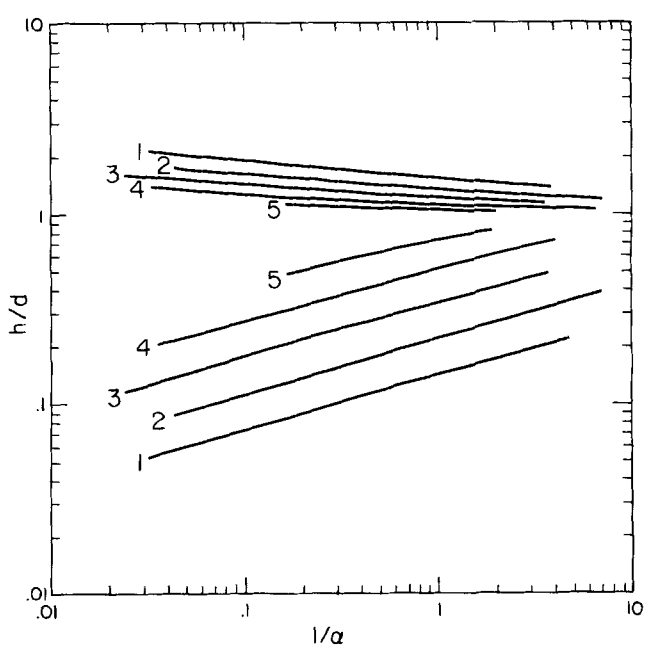

Fig. 2. Minimum film thickness and the maximum thickness of the ripple just upstream from the transition zone for $R = 0$. 1, $d = 10^{-5}$; 2, $d = 10^{-4}$; 3, $d = 10^{-3}$; 4, $d = 10^{-2}$; 5, $d = 10^{-1}$.

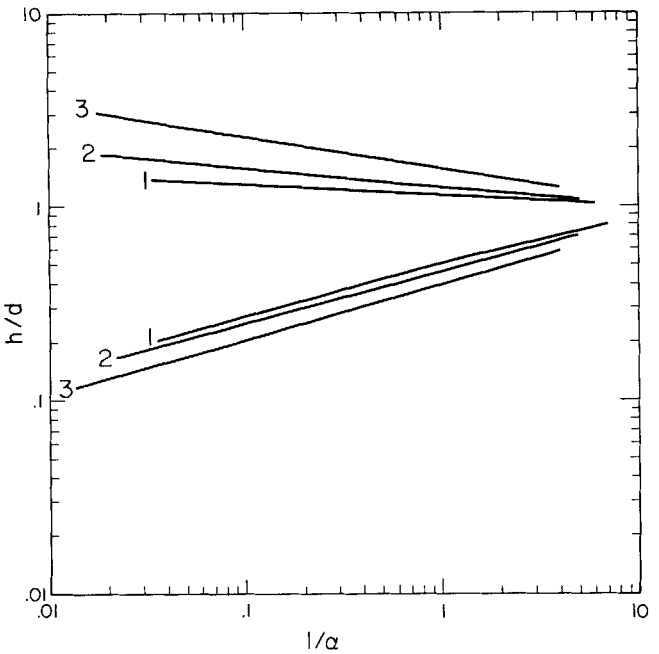

Fig. 3. Minimum film thickness and the maximum thickness of the ripple just upstream from the transition zone for $d = 10^{-2}$. 1, $R = 0$; 2, $R = 100$; 3, $R = 300$.

begins to be a factor and show the initial effects of accelerations. In the case shown, the Reynolds number must be greater than 100 before inertial effects are important, and the minimum film thickness initially decreases as the Reynolds number increases.

DISCUSSION

As the differential Equation (11) is integrated into the region of the static meniscus, h becomes much larger than d. Viscous effects diminish at the rate $(d/h)^3$, and inertial effects diminish almost as quickly. Consequently, the film profile rapidly becomes a static meniscus, and α, which was computed at each step of the integration, becomes a constant. Thus, retaining the dynamic terms even into the hydrostatic region caused no difficulties. Because the wall is stationary with respect to the reservoir, the velocity becomes uniformly small across the film as h/d becomes large. This is an advantage for the approximate solution technique employed here.

All terms of the unsimplified Equations (1) were calculated at several steps during each integration. The terms estimated to be negligible were, in fact, relatively small, and so the approximate solution technique is at least self-consistent.

Wilkes and Nedderman (1962) presented simplified equations which are identical to those given here for the dynamic portions of the flow domain. However, Wilkes and Nedderman linearized the equations about the asymptotic flow upstream and consequently overlooked the transition zone. Moreover, they were unable to generate boundary conditions for the exiting flow and so did not determine it uniquely. Wilkes and Nedderman did, however, consider the case of a stagnant interface. Their approach to this complication can readily be combined with the solution procedure used here.

Bretherton (1961), studying the rise of a long bubble in a capillary tube under the influence of gravity, presented simplified equations for the dynamic and static regions equivalent to those given here. Rather than combine the equations, Bretherton considered the dynamic and static regions separately and patched his two results together. This worked well for the front portion of the bubble, where the flow is from an essentially stagnant and relatively large region into a thin film. Ruschak and Scriven (1977) have recently shown that the method of matched asymptotic expansions can be applied to this type of situation and that there are only two horizontal (cross film) length scales in the limit of small film thickness.

Bretherton's approach is less suited to the rear portion of the bubble, where the flow is from a thin film into a relatively large and essentially stagnant region and where there are three horizontal length scales. In this situation, his differential equation for the film thickness in the dynamic region cannot be integrated to infinity in the downstream direction to obtain a match with the static meniscus. If the method of matched asymptotic expansions is applied, three limits of the problem solution must be examined as film thickness tends to zero. The resulting complications are so great that this approach was abandoned early in the present work. It is not at all clear how Bretherton proceeded at the rear of the bubble; he merely states that his patching scheme can be carried out.

NOTATION

C = $(\sigma/\rho G)^{1/2}$, capillary length
D = upstream film thickness
d = D/C
E = curvature of static meniscus
G = acceleration of gravity
h = film thickness, dimensionless
p = pressure, dimensionless
Q = volumetric flow rate per unit width
u = x component of velocity, dimensionless
v = y component of velocity, dimensionless
X = vertical coordinate
x = X/C
Y = horizontal coordinate
y = Y/C

Greek Letters

α = static meniscus parameter
κ = profile curvature
μ = viscosity
ρ = density
σ = surface tension

LITERATURE CITED

Bretherton, F. P., "The Motion of Long Bubbles in Tubes," *J. Fluid Mech.*, **10**, 166-188 (1961).

Cook, R. A., and R. H. Clark, "An Analysis of the Stagnant Band on Falling Liquid Films," *Ind. Eng. Chem. Fundamentals*, **12**, 106-114 (1973).

Cullen, E. J., and J. F. Davidson, "Absorption of Gases in Liquid Jets," *Trans. Faraday Soc.*, **53**, 113-120 (1957).

Finlayson, B. A., *The Method of Weighted Residuals and Variational Principles*, Academic Press, New York (1972).

Lynn, S., J. R. Straatemeier, and H. Kramers, "Absorption Studies in the Light of the Penetration Theory I," *Chem. Eng. Sci.*, **4**, 49-57 (1955*a*).

Lynn, S., J. R. Straatemeier, and H. Kramers, "Absorption Studies in the Light of the Penetration Theory II," *ibid.*, 58-62 (1955*b*).

Merson, R. L., and J. A. Quinn, "Diffusion and Flow in a Radially Moving Film," *AIChE J.*, **10**, 804-809 (1964).

———, "Stagnation in a Fluid Interface: Properties of the Stagnant Film," *ibid.*, **11**, 391-395 (1965).

Mockros, I. F., and R. B. Krone, "Hydrodynamic Effects on an Interfacial Film," *Science*, **161**, 361-363 (1968).

Nijsing, R. A. T. O., R. H. Hendriksz, and H. Kramers, "Absorpion of CO_2 in Jets and Falling Films of Electrolyte

Solutions, With and Without Chemical Reaction," *Chem. Eng. Sci.*, 10, 88-104 (1959).
Nysing, R. A. T. O. and H. Kramers, "Absorption of CO_2 in Carbonate Bicarbonate Buffer Solutions in a Wetted Wall Column," *ibid.*, 8, 81-89 (1958).
Ruschak, K. J., and L. E. Scriven, "Developing Flow on a Vertical Wall," *J. Fluid Mech.*, 81, 305-306 (1977).
Wilkes, J. O., and R. M. Nedderman, "The Measurement of Velocities in Thin Films of Liquid," *Chem. Eng. Sci.*, **17**, 177-187 (1962).

Manuscript received June 16, 1977; revision received February 13, and accepted March 6, 1978.

Liquid-Solid Mass Transfer in Packed Beds with Downward Concurrent Gas-Liquid Flow

Mass transfer coefficients were determined by measuring the rate of solution of cylindrical 3 or 6 mm benzoic acid tablets into water in the presence of flowing nitrogen, helium, or argon. Gas flow rates varied from 0 to 1.6 kg/(m^2·s) and liquid flow rates from 0.5 to 25 kg/(m^2·s), resulting in hydrodynamic flow patterns varying from trickle to turbulent pulse types of flow. In the pulse regime, the mass transfer coefficient was markedly affected by gas flow rate but did not depend on gas density explicitly if correlated in terms of an energy dissipation function.

CHARLES N. SATTERFIELD
MICHAEL W. VAN EEK
and
GARY S. BLISS

Department of Chemical Engineering
Massachusetts Institute of Technology
Cambridge, Massachusetts 02139

SCOPE

It is necessary to be able to characterize liquid-solid mass transfer in packings representative in size and shape to those encountered in industrial trickle-bed reactors and at gas and liquid flow rates representative of industrial practice in order to understand some of the reasons for the performance of existing reactors and to design and scale-up new reactors.

Until fairly recently, the only information available was a study by van Krevelen and Krekels (1948) in the absence of forced gas flow. During the course of the present work, several other studies were published (Table 1) based in almost all cases on measurements of the rate of solution of a slightly soluble organic material in water in the presence of air or nitrogen. In the present work, mass transfer coefficients were similarly determined by measuring the rate of solution into distilled water of benzoic acid cylindrical tablets, 3 × 3 or 6 × 6 mm in size. However, a wide range of flow conditions was covered, from single phase liquid flow in the presence of stagnant gas to highly pulsing gas-liquid flow. Liquid flow rates were varied from 0.5 to 25 kg/(m^2·s). Gas flow rates were varied from 0 to 1.6 kg/(m^2·s) and encompassed a tenfold variation in gas density by use of helium and argon as well as nitrogen. The mass flow rates of liquid and gas studied encompass essentially the whole range of interest in industrial trickle-bed reactors.

CONCLUSIONS AND SIGNIFICANCE

The nature of the flow regime has a major influence on the rate of mass transfer, and different types of correlations are applicable in different regimes.

Results were obtained in terms of the product $k_S\phi$, where k_S is the liquid-solid mass transfer coefficient, and ϕ, which was not measured separately, is the fraction of the external surface area of the packing that is wetted with flowing liquid. Values of $k_S\phi$ varied by a factor of about 50 over the range of conditions studied and are expressed in terms of a Sherwood number. At a constant gas flow rate and particle size, $k_S\phi$ always increased with increased liquid flow rate. At fixed liquid flow rate and particle size, increasing gas flow rate from zero increased mass transfer by a maximum of only about 10% within the trickle regime but increase to cause pulsing increased mass transfer by a factor of as much as 2.6. A decrease in particle diameter from 6×10^{-3} to 3×10^{-3} m caused an increase in $k_S\phi$ in all flow regimes.

A packed bed may be caused to flood deliberately, for example, by forcing the liquid exiting from the bed to flow upwards through an external tube before allowing it to flow downwards again. At zero or low gas flow rate, when the bed is not caused deliberately to flood, the true hydrodynamic flow pattern may be trickle flow with incomplete or complete wetting, or the bed may instead flood naturally, as shown schematically on Figure 8.

Correlations are presented for predicting mass transfer in the various regimes, and present results are compared and contrasted to previous studies. For incomplete wetting ($Re < 60$), our data and the data of Specchia et al. (1976) for cylinders are correlated by Equation (4). For flooded flow, mass transfer is well predicted by the equation of Carberry (1960) rewritten for cylinders as Equation (3). In the pulse regime, mass transfer coefficients are well described by an energy dissipation function, Equation (13). When thus expressed, the mass transfer coefficient did not depend explicitly on gas density.